

ACEV: Unsupervised Intersecting Manifold Segmentation using Adaptation to Angular Change of Eigenvectors in Intrinsic Dimension

Subhadip Boral, *Student Member, IEEE*, Rikathi Pal, and Ashish Ghosh, *Senior Member, IEEE*

Abstract—Intersecting manifold segmentation has been a focus of research, where individual manifolds, that intersect with other manifolds, are separated to discover their distinct properties. The proposed method is based on the intuition that when a manifold in D dimensional space with an intrinsic dimension of d intersects with another manifold, the data variance grows in more than d directions. The proposed method measures local data variances and determines their vector directions. It counts the number of vectors with non-zero variance, which determines the manifold’s intrinsic dimension. For detection of the intersection region, the method adapts to the changes in the angular gaps between the corresponding direction vectors of the child and parent using exponential moving averages using a tree structure construction. Accordingly, it includes those data points in the same manifold whose neighborhood is within the adaptive angular difference and eventually identifies the data points in the intersection area of manifolds. Data points whose inclusion in the neighborhood-identified data points increases their intrinsic dimensionality are removed based on data variance and distance. The proposed method performs better than 18 SOTA manifold segmentation methods in ARI and NMI scores over 14 real-world datasets with lesser time complexity and better stability.

Index Terms—Manifold, Intrinsic Dimension, Singular Value Decomposition, Exponential Moving Average

I. INTRODUCTION

A manifold [1] is a topological structure that is locally homeomorphic to a Euclidean space of a specific dimension. A multi-manifold structure is a complex arrangement where data points are distributed across multiple distinct manifolds rather than within a single continuous space. Manifold segmentation is a computational task focused on dividing intersecting and non-intersecting manifolds present in data into meaningful and connected segments, aiming to delineate the surface or interior of the manifold using specific criteria. This segmentation process finds applications in diverse fields, including computer graphics, computer vision, medical imaging, and more. There are primarily two types of manifolds: intersecting and non-intersecting. Intersecting manifolds overlap with other manifolds, while non-intersecting manifolds either exist in separate regions of space or are arranged in a manner that prevents intersection. Intersecting Manifold Segmentation holds significant value in various applications, such as medical image analysis, precise segmentation of anatomical structures, and spectral clustering [2]. The primary job of intersecting manifold segmentation is to learn the structure of very individual manifolds and identify the region where it intersects with other manifolds.

Subhadip Boral is with the Department of Computer Science & Engineering, University of Calcutta, Kolkata 700098 and ITER, Siksha O Anusandhan, Bhubaneswar 7501030, India. E-mail: subhadipboral_t@soa.ac.in

Rikathi Pal is with the A.K. Choudhury School of Information Technology, University of Calcutta, Kolkata 700106, India. E-mail: rikathi.pal@gmail.com

Ashish Ghosh is with the International Institute of Information Technology Bhubaneswar, 751003, India. E-mail: ash@isical.ac.in

The next step is to determine which individual manifold the data points in the intersection areas belong to by comparing the structural similarity of the manifold to the data point.

The challenge this intersecting manifold segmentation poses is the identification of data points present in the intersection region. Now the intersecting region may be a region that involves more than two manifolds and therefore determining the number of manifolds present in the region is also a challenging task. The efficacy of two tasks depends on how individual manifold structure is learned by the algorithm because without proper learning the aforementioned tasks are hard to accomplish. The existing works handle the challenges by incorporating different approaches. The works that segment manifolds dependent on the structure of the data fail to learn the structure of the manifold. The other algorithms segment the manifolds depending on the affinity matrices where the formation of affinity matrices is limited to specific assumptions like linear structure, infinite plane, etc. The algorithms that try to understand the tangent structure of the manifold assume that other than the tangent space the data variance is zero. These assumptions fail in real-life scenarios and the performance of the algorithms drops. This encourages the proposed method to segment intersecting manifolds with better efficiency, lesser complexity, and stability. The proposed work, ACEV, is a two-step algorithm, where in the first step the non-intersecting manifolds are segmented and in the next step, individual intersecting manifolds are segmented. ACEV incorporates eigenvalue decomposition of the Laplacian graph matrix for the segmentation of non-intersecting manifolds. ACEV learns the intrinsic dimension of individual manifolds along with their structure and gradual structural changes. The algorithm identifies intersecting areas in a manifold by understanding the abrupt structural change in the neighborhood while traversing the data points and maintaining a tree structure. Then depending on the structural property it determines in which manifold the data points from the intersecting area lie.

The proposed method is an unsupervised manifold segmentation mechanism that initially finds

the non-intersecting manifolds present in a dataset. Now, for each non-intersecting components or manifolds it segments the present intersecting manifolds by studying their intrinsic dimension. By learning the intrinsic dimension, it identifies the data points which lie in intersecting regions. Depending on eigenvalue it filters those data points and includes the data points lying in the exact manifold. The performance and effectiveness of the ACEV eclipses other existing algorithms over 11 datasets. The performance analysis shows the independence of the proposed method over manual parameters. The following sections discuss the state-of-the-art algorithms in this research field, discuss the detailed proposed method, and give a proper performance and comparative analysis. The following sections of the paper include discussions on state-of-the-art algorithms in the research field, provide a detailed explanation of the proposed method, and present a comprehensive performance analysis for comparison.

II. RELATED WORKS

The problem of intersecting manifold segmentation is addressed by various methods, which broadly belong to these categories.

A. Traditional Methods

Methods that do not consider the structure of the individual manifolds and instead of that, segment depending on the local structure of the data. A comparative detail of few these methods are presented in Table I.

B. Manifold Structure Learning Methods

Various methods learn the structure of manifolds and they are used for manifold segmentation. Table II holds the details of these methods.

C. Individual Manifold Structure Learning Based Methods

There are methods dedicated to segment intersecting manifolds with various assumptions and constraints. The brief discussion of these methods are given in Table III.

TABLE I: Comparative discussion on clustering methods for manifold segmentation

Algorithm	Year	Methodology	Dedicated Intersecting Manifold Segmentation	Drawbacks Addressed by ACEV
k means [3]	1988	Clusters datapoints into k clusters by minimizing the distance between datapoints and cluster center.	No	Apriori knowledge of number of manifolds
DBSCAN [4]	1996	Groups closely packed points based on a specified distance threshold and a minimum number of points within the neighborhood.	No	Clustering of data with non-uniform density
BIRCH [5]	1997	Performs hierarchical clustering and reduces the data dimensionality.	No	Apriori knowledge of number of manifolds
OPTICS [6]	1999	Generates a reachability plot to reveal the hierarchical structure of the data.	No	Apriori knowledge of number of manifolds
Mean shift [7]	2005	Clusters by iteratively shifting data points toward the mode of their local density distributions.	No	Apriori knowledge of number of manifolds
Spectral clustering [2]	2011	Clusters data points based on the eigenvectors of the affinity matrix, which is based on Euclidean distances between data points.	No	Segmentation of intersecting structures

TABLE II: Comparative discussion on manifold structure learning methods for manifold segmentation

Algorithm	Year	Methodology	Dedicated Intersecting Manifold Segmentation	Drawbacks addressed by ACEV
Principal component analysis (PCA) [8]	1987	Embeds data points while preserving structural information through data variance.	No	Assumption of linear manifold structure
Locally Linear Embedding (LLE) [9]	2000	Preserves neighborhood-based reconstruction weights during embedding.	No	Non-uniform manifold structure embedding
Multi Manifold Discriminant (MMD Isomap) [10]	2016	Uses class information for manifold segmentation and manifold structure learning. Also embeds each manifold using Isomap.	Yes	Class information based manifold segmentation
Semi-supervised Multi Manifold Isomap (SSMM Isomap) [11]	2018	Learns local linear structure and embeds data points by minimizing intraclass distance and maximizing interclass distance while using partially labeled data.	Yes	Uses class information to understand manifold structure.
UMD Isomap [12]	2022	Captures the non-linear global relationship between data points using Mixture of Probabilistic PCA [13]. Also determines local tangent subspaces to understand the local geometry of the submanifolds.	Yes	Non-adaptive to the structural changes occurred due to the non linearity of the manifold

TABLE III: Comparative discussion on individual manifold structure learning methods

Algorithm	Year	Methodology	Dedicated Intersecting Manifold Segmentation	Drawbacks addressed by ACEV
k -plane clustering (k PC) [14]	2000	Clusters are obtained using hyperplanes constructed by eigenvalue decomposition of the affinity matrix.	No	Assumptions of linear separability of manifolds
k FC [15]	2000	Finds q linear planes which have the minimum Euclidean distance from the datapoints	No	Linear representation of the global structure
Spectral multi-manifold Clustering (SMMC) [16]	2011	Measures cohesion within manifolds and separability between manifolds through tangent space similarity and dissimilarity.	Yes	Fragile manifold structure in the intersection area due to high affinity with other manifolds.
Localized k -flat clustering (Lk FC) [17]	2011	Introduces localized representations of linear models and a distortion measure for cluster quality assessment.	No	Prior assumptions made on linear manifold structure.
k -proximal plane clustering (k PPC) [18]	2013	Finds the best-fit orientation for planar representation of the manifold by maximizing the margin between manifolds.	No	Linear structural representations of non-linear manifolds.
Local k -proximal plane clustering (Lk PPC) [19]	2015	Laplacian graph matrix-based connectivity determination of manifolds.	No	Senses intersecting manifolds as a single manifold.
Twin support vector machine for clustering (TWSVC) [20]	2015	Segments planar representations of K-means derived clusters by incorporating L2 Norm distances.	No	Apriori knowledge of number of manifolds.
TVG+Ambiguity Resolution (TVG+AR) [21]	2015	Zero eigenvalue-based determination of tangents and learning of data variance gap through the exponential moving average helps to segment intersecting manifolds.	Yes	Prior knowledge of intrinsic dimension of the manifold and inefficiency with higher dimensional data.
L1-norm distance minimization based robust TWSVC (RTWSVC) [22]	2017	Improvement of TWSVC by incorporating L1 norm distances.	No	Apriori knowledge of number of manifolds.
k -subspace discriminant clustering (k SDC) [23]	2019	Partition-based clustering of subspaces and learning of local structure through L1 Norm.	No	Segments region of interests instead of manifold structure learning
Multiple flat projections clustering (MFPC) [24]	2021	Local linear projection-based global structure learning and intersecting cluster determination through non-convex optimization.	Yes	Inefficiency while addressing non-uniform manifold structures.
Graph MMC [25]	2023	Uses the Graph Laplacian operator to ensure intramanifold connectivity and intermanifold sparsity	Yes	Aprior knowledge and assumptions about the intersecting manifolds

The existing works are dependent on the user parameters and fail to address major challenges of the field which include sensitivity to data intersections, parameter tuning, and computational complexity. The existing works perform mostly in $O(n^4)$ and $O(n^5)$ which motivates ACEV to perform effectively and efficiently.

III. PROPOSED WORK

A. Problem Statement

Suppose there are n data points represented in D dimensional space and these n data points are lying on $m(\geq 1)$ non-intersecting manifolds, where l_i represents i^{th} non-intersecting manifold. Each l_i consists of $q_i(\geq 1)$ intersecting manifolds and M_{ij} , the j^{th} individual manifold in l_i has intrinsic dimension d_{ij} and $1 \leq i \leq m, 1 \leq j \leq q_i$ and $1 \leq d_{ij} \leq D$. The proposed method first segments those m non-intersecting manifolds and in the second step, it separates each individual manifold M_{ij} , which intersects with other manifolds in l_i if $q_i > 1$, based on an unsupervised approach. This manuscript proposes an innovative approach to this.

B. Segmentation of non-intersecting manifolds

The segmentation of non-intersecting manifolds is based on the work [26], which is an unsupervised manifold segmentation mechanism. The method uses a graph-based component analysis to determine the number of components or non-intersecting manifolds present in the data and uses agglomerative clustering to group data points that belong to the same manifold.

Initially, a k -neighborhood is found for every data point and those k data points are considered adjacent to that data point. Following this mechanism an adjacency matrix is created which resembles a graph. There are n data points and therefore an $n \times n$ adjacency matrix G will be obtained. The method follows the idea that the singular value decomposition of a Laplacian graph matrix will depict the number of disjoint components present in the graph. In other words, the number of eigenvectors with corresponding zero eigenvalues of the Laplacian

graph matrix will be the number of components in the graph. Therefore, the number of components present in the graph is found by constructing the adjacency matrix G and corresponding Laplacian graph matrix L_G . In other words, as there are m non-intersecting manifolds present in the dataset, the number of components in the graph G will be also m and the number of eigenvectors with corresponding zero eigenvalues of the Laplacian graph matrix will be m . The Laplacian graph matrix L_G corresponding to the adjacency matrix G will be a $n \times n$ matrix where value of the j th column of the i th row will be

$$\chi_{ij} = \begin{cases} -1 & \text{if } v_i \text{ and } v_j \text{ are adjacent} \\ d(v_i) & \text{if } i = j \\ 0 & \text{otherwise;} \end{cases} \quad (1)$$

where v_i and v_j are the i -th and j -th vertex and $d(v_i)$ is degree of v_i . Then singular value decomposition (SVD) of the Laplacian graph matrix L_G is performed and the number of zero eigenvalues is counted.

Now to find which datapoint is part of which non-intersecting manifold, hierarchical agglomerative clustering [27] is performed on the data. This yields m clusters, where each cluster represents individual non-intersecting manifolds l_i and the proposed method finds the intersecting manifolds present in each l_i .

C. Segmentation of intersecting manifolds

The proposed method introduces a novel unsupervised intersecting manifold segmentation mechanism. In Figures 1a and 1b, data points A and B are attributed to manifold U , data points C and D to manifold V , while data points P, Q and R reside within the intersection of these two manifolds. The primary objective is to identify the data points situated in the intersection region of different manifolds with an approach that relies on the intrinsic dimension [28] of individual manifolds. As depicted in Figures 1a and 1b, manifolds U and V have an intrinsic dimension 2 and this is true for data points A, B, C , and D as their local

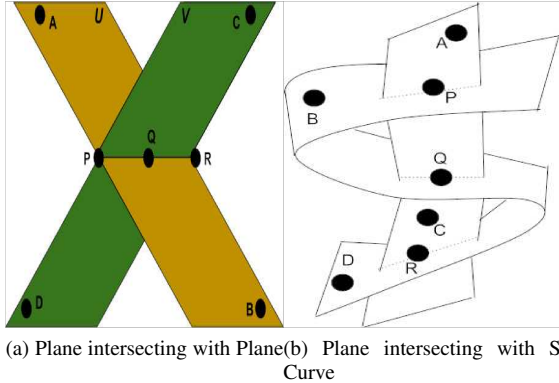


Fig. 1: Synthetic intersecting manifold structure

neighbourhood properties can be accounted in 2-D space without information loss. However, data points P, Q and R possess an intrinsic dimension of 3 as these lie in the intersection region and local neighbourhood properties can not be accounted in less than 3-D space without information loss.

This signifies that the algorithm must learn the intrinsic dimension of individual manifold M_{ij} . Once learned, the algorithm can identify the data points that belong to the intersection region by comparing the intrinsic dimension. If the algorithm determines the intrinsic dimension of the manifold as d , data points in the intersection region will have an intrinsic dimension $> d$ as there will be more information that can not be accounted for in d -dimensional space due to the inclusion of data points from another manifold in their neighbourhood. The following learning process outlines the steps required to accomplish this task.

1) *Intrinsic Dimension Determination*: Suppose there is a d -dimensional manifold in a D ($D > d$)-dimensional vector space and the neighbourhood of a data point t from that manifold is considered. Now, the covariance matrix of that neighbourhood is computed and D eigenvalues and associated D eigenvectors are found. The number of eigenvectors corresponding to non-zero eigenvalues for that neighbourhood will be d . This is true because there will be zero data variance in the other $(D - d)$ directions, which means that the associated eigen-

values will be zero. Further in the discussion, eigenvector and eigenvalues, eigenvector and eigenvalues of the datapoint and eigenvector and eigenvalue of the neighbourhood will mean eigenvectors and eigenvalues of the covariance matrix of that data point's neighbourhood. The algorithm determines the directions of the eigenvectors with non-zero eigenvalues for the neighbourhood of t . Suppose, two data points t and f belong to the same manifold, then their neighbourhood structure will be similar and the direction of data variance will be similar and therefore, their corresponding directions of eigenvectors will be similar, i.e., g^{th} principal component of datapoints t and f will be in the same direction. Therefore, the angular gap between two corresponding eigenvectors derived from the neighbourhood of two individual data points is decisive in determining whether those two data points belong to the same local structure or not. So, the angular gaps between the corresponding eigenvectors of the data points are calculated using equation 2 for the data point t and f , where \vec{p}_{tg} and \vec{p}_{fg} are the g^{th} principal component of t^{th} and f^{th} data point respectively.

$$angle_diff_fer_g(t, f) = \cos^{-1} \left(\frac{\langle \vec{p}_{tg}, \vec{p}_{fg} \rangle}{\|\vec{p}_{tg}\| \cdot \|\vec{p}_{fg}\|} \right),$$

$$g = 1, \dots, D \quad (2)$$

In Figure 2, the green circles show the neighbourhoods of data points E and C , while the red circle corresponds to the neighbourhood of datapoint Q . The arrows within each circle denote the direction of non-zero data variance for their respective neighbourhoods, where the arrow length is independent of the amount of data variation. The angular difference between the 1st principal components of datapoints E and C is denoted by α and the same is denoted by β for the 2nd principal components as shown in Figure 2. For datapoints E and C , α and β are observed to be nearly zero as the neighbourhood structures are similar. However, for datapoint Q , the angular difference in the third direction is high, as Q is from a region which has an intrinsic dimension of 3. It will have a non-similar 3rd eigenvector

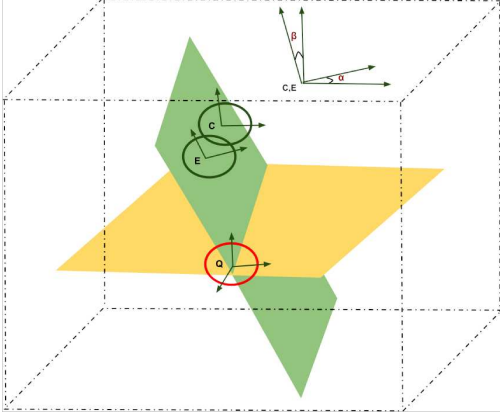


Fig. 2: Neighborhood (using circles) and direction of data variance (using arrows) representation of individual data points

direction when compared with the corresponding eigenvector direction of E or C . This gap indicates a distinct structural dissimilarity compared to the other two datapoints and this signifies the change in intrinsic dimensionality.

The mechanism mentioned above captures the intrinsic dimension of local structure, i.e., neighbourhood of data points. This also emphasizes the fact that with non-significant $angle_diff_g(t, f), \forall g$ ACEV should include f in the same manifold as t . However, a manifold exhibits a local resemblance to Euclidean space while forming a non-linear structure globally. Therefore, the local structural differences may be non-significant but not uniform across the entire space. Therefore, the proposed method must learn the change in the local structure in terms of angular gap and this local structural change is caused by the global non-linearity of the manifold. The algorithm learns the changes in the angular gap between eigenvectors to address this problem.

2) *Manifold Structure Learning using Time Series Analysis*: These local structural changes manifest gradually rather than abruptly. To effectively learn the change in angular differences, ACEV employs a neighbourhood-based approach using the Exponential Moving Average (EMA) method [29]. The EMA method is applied through the following

equation 3. This strategic use of EMA ensures that the algorithm adapts to the evolving nature of local structures and captures the subtle variations in the angular gaps between eigenvectors. The predicted angular gap is computed as

$$E_d(s) = \alpha \cdot angle_diff_d(s, s-1) + (1 - \alpha) \cdot E_d(s-1) \quad (3)$$

where $E_d(s)$ predicts the angular difference of d th eigenvector for s th data point, α is the exponential smoothing factor and $d = 1 \dots D$.

To segment intersecting manifolds, ACEV initiates traversal from a data point $t \in l_i$, where $t = \min(t_1, \dots, t_{n_i})$ for any one dimension in D and n_i is the number of unlabelled data points in l_i which are not included in any individual manifold. t is first considered for the manifold and serves as the root. After determining t , its k -nearest neighbor data points are identified for traversal and probable inclusion as its children. The algorithm aims to include data points within the same manifold that exhibit non-significant angular differences in all directions. It begins by finding the eigenvectors of the neighbourhood for both the parent $s-1$ and potential child data points s . Subsequently, it calculates the angular differences $angle_diff_g(s, s-1)$ between these vectors using equation 2. ACEV then predicts angular differences $E_d(s)$ for all directions using equation 3. If the difference between $E_d(s)$ and $angle_diff_d(s, s-1)$ is insignificant for all D directions, then the potential child is included in the same manifold as the parent.

The inclusion process follows a depth-first search method, creating a tree structure with t as the root. The calculation of equation 3 follows the path from the root to the specific data point s for which it is calculated and $s-1$ is the parent of s and so on in the tree structure. This inclusion procedure continues until each data point in l_i is included, or with the current neighbourhood, the probable child s couldn't be included.

It is important to mention that the EMA method requires an initial construction phase and therefore, 0.05% of unlabelled data points are included in the tree without constraint. This step has negligible

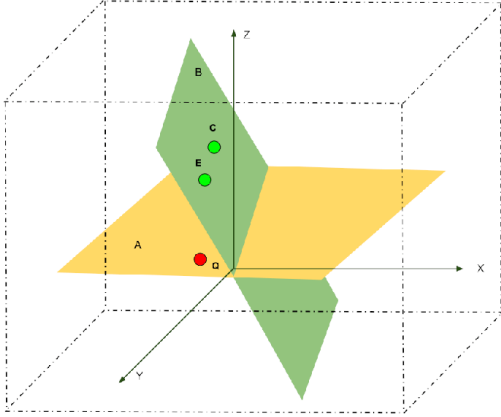


Fig. 3: Eigenvalue and distance-based neighbourhood filtration

significance due to the inclusion of only 0.05% of unlabelled data points and due to adaptation effect the effect also fades.

3) *Intersecting Neighbourhood Filtration*: The unsatisfiability of the inclusion criterion signifies that there are data points in the neighbourhood, for which there is a significant angular difference in one or more directions. This establishes that there is an increase in data variance in these directions, i.e., there is an increase in eigenvalue. It is evident that the probable child is lying in the intersection region and ACEV filters the neighbourhood and considers those data points lying on that particular manifold that it is currently traversing and excludes those data points from other manifolds.

For example as shown in Figure 3, suppose \vec{X} , \vec{Y} and \vec{Z} are the directions of data variance of Q , which lies on manifold A , and data points C and E are wrongly included in the neighbourhood of Q and Q couldn't be included in the manifold A . As Q lies in manifold A , there will be zero eigenvalues in the direction of Z ; therefore, the predicted angular gap in that direction will be nearly zero.

Now, consider the distances of Q , C and E from \vec{X} , \vec{Y} and \vec{Z} . It is clear that Q will be very close to \vec{X} and \vec{Y} rather than C and E , but may have similar distances from \vec{Z} . In this scenario, for the removal of C and E from the neighbourhood of Q , eigenvector directions and associated eigenvalues

of the covariance matrix of the neighbourhood of $(Q - 1)$, the parent of Q , will be beneficial. Let us consider the modified distance for each data point r in the neighbourhood of Q shown in the equation 4.

$$mod_dis(r) = \sum_{w=1}^D dis(e_w, r) \frac{E_w(r)}{E_w(Q-1)}. \quad (4)$$

where $dis(e_w, r)$ is the distance of datapoint r from w th eigenvector of neighbourhood of $(Q-1)$. $E_w(r)$ is eigenvalue for w th eigenvector of neighbourhood of r and $E_w(Q-1)$ is eigenvalue for w th eigenvector of neighbourhood of $(Q-1)$. The data points, which are on the same manifold, will have similar $E_w(r)$ with $E_w(Q-1)$, $\forall w$ and $\frac{E_w(r)}{E_w(Q-1)}$ will be nearly 1. In contrast, the data points which are not on the same manifold will have dissimilar values $E_w(r)$ with $E_w(Q-1)$ and $\frac{E_w(r)}{E_w(Q-1)}$ will be more than 1. For example, in Figure 3, C will have a higher variance in \vec{Z} direction, i.e., $E_{\vec{Z}}(C)$ will be higher than $E_{\vec{Z}}(Q-1)$ and $\frac{E_{\vec{Z}}(C)}{E_{\vec{Z}}(Q-1)}$ will be greater than 1. This will be the contribution of $\frac{E_w(r)}{E_w(Q-1)}$ in demarcation. Similarly, the data points, which are not part of the manifold, may have similar $E_w(r)$ with $E_w(Q-1)$ but as they are not from the same manifold the value of $dis(e_w, r)$ will be higher than a data point which lies on that manifold. This will be the contribution of $dis(e_w, r)$ in demarcation. So, the $mod_dis(r)$ for neighbourhood data points of Q which are on manifold A will be comparatively lower than data points C and E .

So using this intuition to filter the neighbourhood, $mod_dis(r)$ is found for every data point in the neighbourhood of the probable child Q . Now, maintaining a decreasing order of $mod_dis(r)$, the ACEV removes data points from the neighbourhood of Q one by one and calculates the angular differences $angle_diff_fer_d(Q, Q-1)$, $\forall d$ using equation 2 with the updated neighbourhood. If the difference between $E_d(Q)$ and $angle_diff_fer_d(Q, Q-1)$ is insignificant for all directions D , the potential child Q is included in the same manifold as the child. Removal of certain data points will satisfy the criterion, and Q will be included with this updated neighbourhood and the traversal and inclusion of

data points continue. This is how the ACEV finds individual manifolds and continues to search for manifolds in every non-intersecting component l_i until all the data points become part of a manifold.

Figure 4 represents a concise workflow of ACEV. There are four intersecting manifolds, which belong to two non-intersecting manifolds. So, in the first step, two non-intersecting manifolds are separated. Next, considering one of them, the s-curve and line, ACEV starts segmenting intersecting ones. Initial 0.05% of data points are labelled unconditionally and then, data points are included maintaining EMA-dependent angular gap and intersecting regions are detected. Upon detection, ACEV filters the neighbourhood, includes data points, and continues until no unlabelled data point can be included. Then, the next manifold is segmented without hindrance as the other intersecting manifold is labelled. For the other non-intersecting manifold, two individuals are segmented and ultimately, the four manifolds are segmented.

D. Algorithm and Time Complexity Analysis

The algorithm involves several steps: firstly, $O(nD \log(n))$ is needed to construct the tree-like structure of k -neighborhoods. Subsequently, $O(n^3)$ is required for labeling and segmenting non-intersecting manifolds. Finding the k nearest neighbor of the root data point takes $O(k \log(n))$ time, followed by determining the principal axis, which consumes $O(n^3)$ time involving covariance matrix computation and eigenvector calculation. The angle between vectors is found in $O(D)$ time, where D is the number of dimensions. Since, the algorithm runs recursively for each neighbor, the time required for each recursion is $\log_k n$. The overall time complexity of the ACEV is expressed as $O(nD \log(n) + n^3 + \log_k n(k \log(n) + n^3 + D))$. It's noteworthy that the complexity is expected to decrease over time as manifold determination reduces the number of data points, denoted as n .

IV. PERFORMANCE ANALYSIS AND COMPARATIVE STUDY

A. Experimental Setup and Performance Evaluation Metrics

The performance analysis and comparative study were carried out on an Intel *i5* processor with a clock speed of 4.90 GHz and 16 gigabytes of RAM without a dedicated graphics processing unit. The effectiveness of the proposed method is examined using real-life datasets with diverse sample sizes, dimensions, and classes. Table IV contains the description of each dataset. The exponential smoothing factor α was set to 0.6 and the k -neighborhood value were employed for individual datasets with $k = 25$.

TABLE IV: DESCRIPTION OF THE BENCHMARK DATASETS

Sl No.	Dataset	Samples	Dimension	Classes
1	Ecoli [30]	336	7	8
2	Wine [31]	178	13	3
3	Car[32]	1728	6	4
4	Echocardiogram [33]	131	10	2
5	Ionosphere [34]	351	33	2
6	Hepatitis [35]	155	19	2
7	Zoo [36]	101	16	7
8	Seeds [37]	210	7	3
9	Australia [38]	690	14	2
10	Iris [39]	150	4	3
11	Letter [40]	20000	16	12
12	DNA [41]	2000	180	3
13	Isolet [42]	7797	617	26
14	Swarm Behaviour [43]	24017	2400	2

For the evaluation of the performance of ACEV and the related state-of-the-art models, Adjusted Rand Index (ARI) [44] and Normalized Mutual Information (NMI) [45] metrics have been used. These metrics assess the clustering efficiency by comparing the algorithm-determined clusters with the ground truth or reference clusters. The ARI considers the randomness in data point assignment to clusters and quantifies the clustering algorithm's ability to capture the true structure of the data. ARI ranges from -1 to 1 , where 1 indicates a perfect match, 0 suggests randomness and negative values imply clustering worse than random. NMI measures mutual information between true and predicted clustering. It normalizes the result between 0 and 1 , considering the entropy of individual and

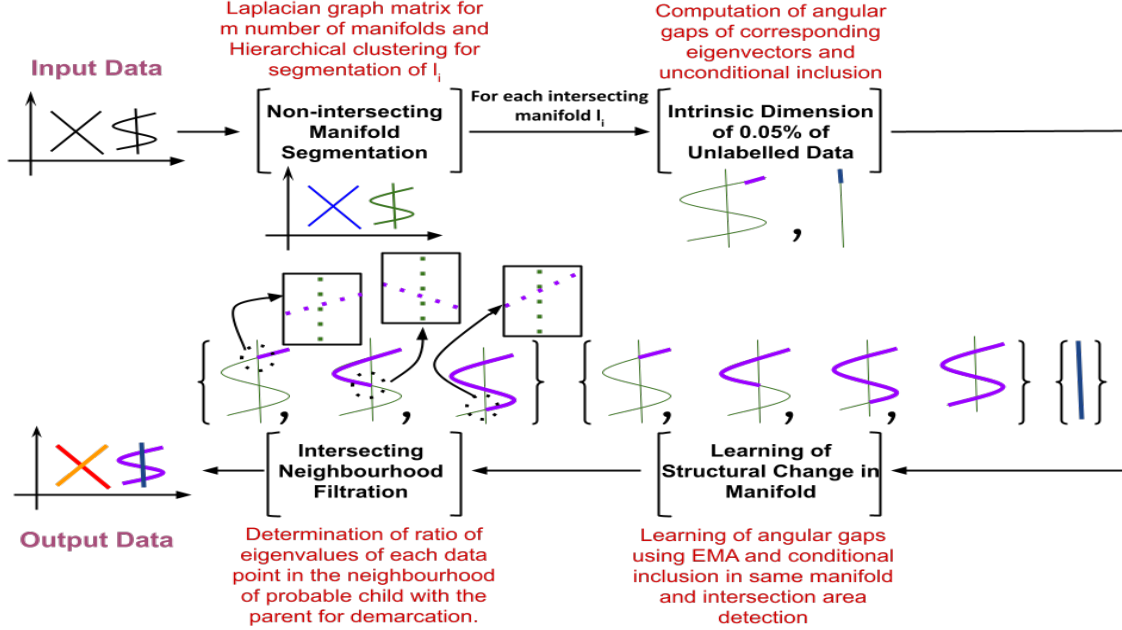


Fig. 4: Graphical workflow of the proposed method ACEV

joint clusterings. NMI ranges from 0 to 1, with higher values indicating better results.

Two statistical analyses are considered to evaluate the qualitative development of ACEV. The Friedman test [46] checks for performance differences among groups of ordinal data and calculates a Friedman statistic based on ranked data and the statistic is compared with the chi-squared distribution. If the calculated p-value is below the significance level (0.05) then the null hypothesis of no significant differences among groups is rejected and indicates dissimilarity. The Wilcoxon signed-rank test [47] is used to ascertain whether ACEV's performance differs significantly from each of the other models if the Friedman test indicates that there are differences between the models. The Wilcoxon rank test compares paired observations to find significant differences. It involves the ranking of absolute differences between paired observations. The test statistic is calculated by summing the ranks of positive and negative differences separately. The

p-value is then compared with the critical value 0.05 to decide whether to reject the null hypothesis of no significant difference.

B. Performance Analysis and Sensitivity Study on Parameters

The proposed method consists of two components: the first focuses on segmenting non-intersecting manifolds, and the second on intersecting manifolds. Table V highlights the necessity of both parts, with non-intersecting manifold segmentation excelling for datasets Echocardiogram, Zoo, and Seeds, while intersecting manifold segmentation performs better for other datasets. Notably, ACEV consistently outperforms both individual approaches and highlights the necessity of incorporating both intersecting and non-intersecting manifold segmentation to achieve proper segmentation.

The efficacy of the ACEV depends on three key factors: k , α , and the learning percentage. To assess its performance across these parameters, Figure 5,

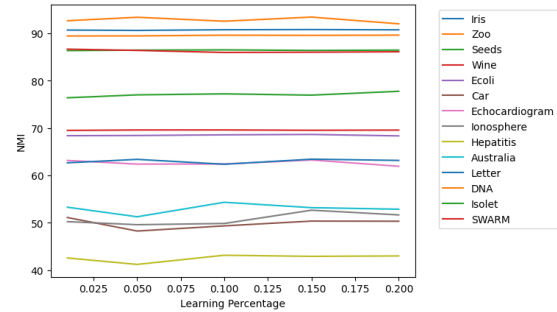
TABLE V: Comparative Analysis of Individual Segmentation Mechanism with ACEV

Sl No.	Non-Intersecting		Intersecting		ACEV	
	ARI	NMI	ARI	NMI	ARI	NMI
1	0.48	0.32	0.61	0.37	0.81	0.68
2	0.45	0.35	0.50	0.32	0.80	0.69
3	0.39	0.25	0.42	0.30	0.68	0.50
4	0.64	0.40	0.59	0.38	0.89	0.63
5	0.58	0.32	0.59	0.38	0.72	0.50
6	0.38	0.29	0.40	0.32	0.64	0.43
7	0.7	0.56	0.66	0.50	0.9	0.89
8	0.69	0.54	0.68	0.52	0.87	0.863
9	0.56	0.29	0.59	0.30	0.7	0.54
10	0.62	0.65	0.78	0.63	0.89	0.9
11	0.54	0.32	0.57	0.39	0.78	0.63
12	0.65	0.43	0.72	0.69	0.97	0.93
13	0.53	0.41	0.58	0.53	0.75	0.77
14	0.48	0.51	0.53	0.61	0.84	0.86

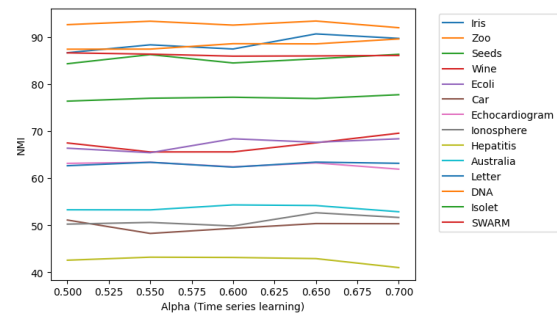
and 6 illustrate the algorithm’s behavior over a specified range for each variable. The algorithm indeed demonstrates robustness with minimal training requirements, as evidenced by the ablation study which indicates stability and independence across varying learning percentages. Notably, the algorithm’s performance remains unaffected by the exponential smoothing factor and exhibits resilience to changes in the neighbourhood parameter. The latter, although recognized as an open research problem due to the delicate balance required for optimal performance, showcase the algorithm’s effectiveness, as it operates reliably over a range of nearest-neighbor values. High values of k are noted for potentially compromising the locally linear property of the manifold, while excessively low values risk generating disconnected components. Despite these challenges, the ACEV performs consistently and effectively, making it less vulnerable to fluctuations in the nearest neighbour parameter.

C. Comparative Analysis

ARI and NMI scores have been computed for 18 state-of-the-art intersecting manifold segmentation algorithms across real-life datasets. The performance of comparative methods and ACEV are presented in Tables VI and VII. In these tables, the best-performing algorithm is highlighted in green for each dataset, while the second-best is colored



(a) Performance dependency on training phase



(b) Performance dependency on exponential smoothing factor

Fig. 5: Sensitivity analysis of ACEV on two parameters

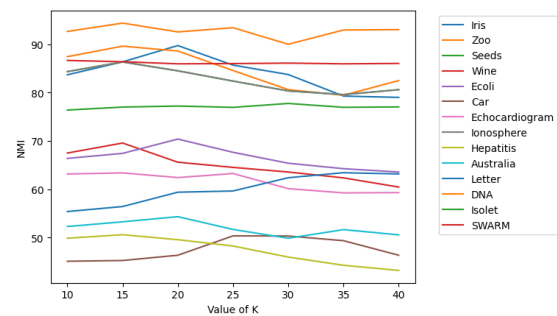


Fig. 6: Performance dependency on nearest neighbor parameter



Fig. 7: Dependency on neighbourhood construction for labelling co-existing concave and convex surface in same manifold

yellow. Notably, the ACEV consistently outperforms others, and even when it is the second-best, the performance is very close to the top algorithm.

Following this, a Friedman test was conducted using ARI and NMI scores. The obtained p-values for ARI and NMI were 7.52×10^{-16} and 2.16×10^{-18} , respectively. These significantly low p-values indicate that clustering algorithms differ significantly. The last row of Tables VI and VII presents the results of the Wilcoxon rank test, emphasizing the significant difference of the proposed method from others. This signifies that the performance of ACEV is stable over these datasets whereas other methods sometimes outperform ACEV for a few datasets.

V. DISCUSSION

An implicit assumption of the algorithm is that change in the tangent space should be smooth which may not be always satisfied. For example, if there is a concave part on a generally convex surface, then there is an abrupt change in the tangent direction as shown in Figure 7. The proposed algorithm using EMA will learn the structural change in the tangent space shown in red in Figure 7 by learning the local structures *A*, *B*, and *C* gradually and include them in the same manifold. This will depend on the neighbourhood construction because if it creates a neighbourhood like *D* then there will be a significant difference in the tangent space and it will not be labelled as the same manifold. So the dependency of the algorithm like other existing algorithms on the neighborhood construction is a limitation.

VI. CONCLUSION AND FUTURE WORK

The proposed two-step intersecting manifold segmentation mechanism (ACEV) learns the intrinsic

TABLE VI: Comparative Performance Analysis of State-of-the-art Methods and ACEV Using Adjusted Rand Index (ARI) Scores

SL No.	Imeans	Mean Shift	Optics	Birch	DBSCAN	SMMC	KPC	KPPC	LKPPC	TWSSVC	KFC	LKFC	RTWSSVC	KSDC	UMD Isomap	Graph MMC	TVG+AR	MIFPC	ACEV
1	0.70	0.63	0.41	0.50	0.46	0.50	0.51	0.51	0.54	0.82	0.70	0.54	0.52	0.77	0.65	0.72	0.56	0.86	0.81
2	0.68	0.51	0.39	0.45	0.50	0.69	0.51	0.52	0.71	0.67	0.67	0.68	0.66	0.66	0.74	0.68	0.49	0.77	0.80
3	0.54	0.50	0.41	0.49	0.45	0.51	0.52	0.56	0.58	0.53	0.54	0.60	0.54	0.54	0.55	0.56	0.39	0.61	0.68
4	0.68	0.61	0.50	0.56	0.57	0.76	0.73	0.73	0.73	0.50	0.72	0.72	0.73	0.68	0.76	0.70	0.39	0.86	0.89
5	0.57	0.50	0.36	0.48	0.40	0.67	0.61	0.53	0.59	0.50	0.70	0.60	0.66	0.57	0.53	0.56	0.35	0.59	0.72
6	0.51	0.53	0.45	0.51	0.47	0.49	0.47	0.52	0.50	0.50	0.52	0.50	0.63	0.50	0.49	0.52	0.50	0.52	0.64
7	0.81	0.73	0.60	0.59	0.62	0.78	0.61	0.75	0.85	0.83	0.85	0.91	0.61	0.84	0.73	0.73	0.44	0.96	0.90
8	0.85	0.70	0.55	0.60	0.45	0.81	0.72	0.60	0.84	0.65	0.72	0.85	0.72	0.85	0.69	0.72	0.53	0.94	0.86
9	0.50	0.45	0.29	0.35	0.30	0.50	0.49	0.50	0.50	0.50	0.52	0.50	0.49	0.50	0.60	0.62	0.44	0.61	0.70
10	0.86	0.79	0.60	0.74	0.45	0.85	0.63	0.56	0.95	0.90	0.90	0.87	0.91	0.89	0.74	0.76	0.62	0.98	0.89
11	0.68	0.63	0.51	0.60	0.55	0.53	0.50	0.51	0.74	0.56	0.62	0.68	0.60	0.63	0.63	0.65	0.62	0.76	0.78
12	0.63	0.60	0.46	0.54	0.50	0.75	0.75	0.69	0.56	0.74	0.76	0.56	0.74	0.56	0.81	0.83	0.57	0.96	0.97
13	0.53	0.50	0.45	0.49	0.42	0.80	0.70	0.59	0.68	0.63	0.65	0.63	0.66	0.59	0.58	0.60	0.45	0.67	0.85
14	0.60	0.54	0.50	0.52	0.54	0.61	0.49	0.53	0.73	0.66	0.74	0.73	0.69	0.78	0.70	0.71	0.40	0.80	0.84
P-Value	.000122	0.0001207	0.0001207	0.0001207	0.0001207	0.000366	0.000122	0.000122	0.00671387	0.000610352	0.00024414	0.003051558	0.000366211	0.00024414	0.00012204	0.000122	0.00012304	0.00012304	0.02121094

TABLE VII: Comparative Performance Analysis of State-of-the-art Methods and ACEV Using Normalized Mutual Information (NMI) Scores

SL No.	Imwans	Mean Shift	Optics	Birch	DBSCAN	SMMC	KPC	KPRC	LKPRC	TWSVC	KFC	LKFC	RWSVC	KSVC	UMD Isomap	GraphMMC	TVG-LAR	MPRC	ACEV
1	0.59	0.52	0.48	0.50	0.36	0.16	0.21	0.66	0.58	0.52	0.65	0.70	0.61	0.60	0.51	0.43	0.43	0.65	0.69
2	0.42	0.38	0.43	0.40	0.34	0.39	0.68	0.52	0.47	0.49	0.43	0.34	0.45	0.40	0.58	0.53	0.35	0.45	0.69
3	0.33	0.20	0.15	0.18	0.10	0.11	0.68	0.19	0.31	0.18	0.14	0.28	0.16	0.19	0.39	0.44	0.34	0.50	0.50
4	0.32	0.30	0.30	0.25	0.23	0.48	0.58	0.05	0.41	0.09	0.39	0.39	0.45	0.37	0.52	0.51	0.44	0.67	0.63
5	0.12	0.25	0.22	0.20	0.21	0.27	0.14	0.05	0.13	0.02	0.31	0.26	0.26	0.11	0.38	0.46	0.25	0.13	0.50
6	0.003	0.02	0	0.05	0	0	0.01	0.09	0.03	0.003	0.008	0.004	0.15	0.005	0.28	0.37	0.29	0.07	0.43
7	0.73	0.60	0.49	0.52	0.50	0.73	0.50	0.57	0.78	0.74	0.80	0.82	0.50	0.77	0.61	0.64	0.64	0.893	0.898
8	0.70	0.59	0.55	0.50	0.45	0.64	0.51	0.20	0.72	0.42	0.52	0.69	0.52	0.66	0.69	0.56	0.42	0.83	0.86
9	0.03	0.10	0.05	0.02	0.07	0.03	0.32	0.01	0.02	0.02	0.02	0.02	0.008	0.02	0.04	0.49	0.42	0.24	0.54
10	0.75	0.65	0.60	0.66	0.62	0.76	0.25	0.13	0.88	0.83	0.80	0.77	0.82	0.77	0.68	0.73	0.66	0.94	0.90
11	0.42	0.40	0.35	0.41	0.39	0.20	0.01	0.05	0.54	0.25	0.34	0.42	0.43	0.33	0.54	0.56	0.37	0.56	0.63
12	0.36	0.45	0.40	0.47	0.42	0.48	0.55	0.58	0.42	0.58	0.70	0.91	0.58	0.91	0.72	0.74	0.59	0.91	0.93
13	0.40	0.31	0.35	0.32	0.29	0.48	0.45	0.51	0.62	0.55	0.62	0.50	0.61	0.52	0.59	0.70	0.42	0.64	0.77
14	0.52	0.49	0.40	0.42	0.35	0.61	0.59	0.39	0.71	0.40	0.66	0.65	0.66	0.75	0.73	0.77	0.42	0.82	0.86
P-Value	0.000122	0.00012207	0.00012207	0.00012207	0.00012207	0.000122	0.000122	0.00012207	0.00012207	0.00012207	0.00012207	0.00012207	0.00012207	0.00012207	0.00012206	0.00012207	0.000122	0.0012273	0.0012273

dimension of individual manifolds and segments them from each other manifolds and demonstrates notable efficiency gain over existing methods with better time complexity. The unsupervised segmentation capability makes ACEV well-suited for practical applications in real-life scenarios. Along with these positivities, the limitation will be reduced for betterment in the future.

REFERENCES

- [1] F. Anwar, S. Sadaoui, and B. Selim, "Conceptual and empirical comparison of dimensionality reduction algorithms (pca, k pca, lda, mds, svd, lle, isomap, le, ica, t-sne)," *Computer Science Review*, vol. 40, p. 100378, 2021.
- [2] Y. Wang, Y. Jiang, Y. Wu, and Z.-H. Zhou, "Spectral clustering on multiple manifolds," *IEEE Transactions on Neural Networks*, vol. 22, no. 7, pp. 1149–1161, 2011.
- [3] A. K. Jain and R. C. Dubes, *Algorithms for clustering data*. Prentice-Hall, Inc., 1988.
- [4] M. Ester, H.-P. Kriegel, J. Sander, X. Xu *et al.*, "A density-based algorithm for discovering clusters in large spatial databases with noise," in *kdd*, vol. 96, no. 34, 1996, pp. 226–231.
- [5] T. Zhang, R. Ramakrishnan, and M. Livny, "Birch: A new data clustering algorithm and its applications," *Data mining and knowledge discovery*, vol. 1, pp. 141–182, 1997.
- [6] M. Ankerst, M. M. Breunig, H.-P. Kriegel, and J. Sander, "Optics: Ordering points to identify the clustering structure," *ACM Sigmod record*, vol. 28, no. 2, pp. 49–60, 1999.
- [7] K. G. Derpanis, "Mean shift clustering," *Lecture Notes*, vol. 32, pp. 1–4, 2005.
- [8] S. Wold, K. Esbensen, and P. Geladi, "Principal component analysis," *Chemometrics and intelligent laboratory systems*, vol. 2, no. 1-3, pp. 37–52, 1987.
- [9] S. T. Roweis and L. K. Saul, "Nonlinear dimensionality reduction by locally linear embedding," *science*, vol. 290, no. 5500, pp. 2323–2326, 2000.
- [10] B. Yang, M. Xiang, and Y. Zhang, "Multi-manifold discriminant isomap for visualization and classification," *Pattern Recognition*, vol. 55, pp. 215–230, 2016.
- [11] Y. Zhang, Z. Zhang, J. Qin, L. Zhang, B. Li, and F. Li, "Semi-supervised local multi-manifold isomap by linear embedding for feature extraction," *Pattern Recognition*, vol. 76, pp. 662–678, 2018.
- [12] X. Gao, J. Liang, W. Wang, X. Bai, and L. Jia, "An unsupervised multi-manifold discriminant isomap algorithm based on the pairwise constraints," *International Journal of Machine Learning and Cybernetics*, vol. 13, no. 5, pp. 1317–1336, 2022.
- [13] M. E. Tipping and C. M. Bishop, "Mixtures of probabilistic principal component analyzers," *Neural computation*, vol. 11, no. 2, pp. 443–482, 1999.
- [14] P. S. Bradley and O. L. Mangasarian, "K-plane clustering," *Journal of Global optimization*, vol. 16, pp. 23–32, 2000.
- [15] P. Tseng, "Nearest q-flat to m points," *Journal of Optimization Theory and Applications*, vol. 105, pp. 249–252, 2000.

- [16] Y. Wang, Y. Jiang, Y. Wu, and Z.-H. Zhou, "Spectral clustering on multiple manifolds," *IEEE Transactions on Neural Networks*, vol. 22, no. 7, pp. 1149–1161, 2011.
- [17] —, "Localized k-flats," in *Proceedings of the AAAI Conference on Artificial Intelligence*, vol. 25, no. 1, 2011, pp. 525–530.
- [18] Y.-H. Shao, L. Bai, Z. Wang, X.-Y. Hua, and N.-Y. Deng, "Proximal plane clustering via eigenvalues," *Procedia Computer Science*, vol. 17, pp. 41–47, 2013.
- [19] Z.-M. Yang, Y.-R. Guo, C.-N. Li, and Y.-H. Shao, "Local k-proximal plane clustering," *Neural Computing and Applications*, vol. 26, pp. 199–211, 2015.
- [20] Z. Wang, Y.-H. Shao, L. Bai, and N.-Y. Deng, "Twin support vector machine for clustering," *IEEE transactions on neural networks and learning systems*, vol. 26, no. 10, pp. 2583–2588, 2015.
- [21] S. Deutsch and G. G. Medioni, "Intersecting manifolds: detection, segmentation, and labeling," in *Twenty-Fourth International Joint Conference on Artificial Intelligence*, 2015.
- [22] Q. Ye, H. Zhao, Z. Li, X. Yang, S. Gao, T. Yin, and N. Ye, "L1-norm distance minimization-based fast robust twin support vector k -plane clustering," *IEEE transactions on neural networks and learning systems*, vol. 29, no. 9, pp. 4494–4503, 2017.
- [23] C.-N. Li, Y.-H. Shao, Y.-R. Guo, Z. Wang, and Z.-M. Yang, "Robust k-subspace discriminant clustering," *Applied Soft Computing*, vol. 85, p. 105858, 2019.
- [24] L. Bai, Y.-H. Shao, Z. Wang, W.-J. Chen, and N.-Y. Deng, "Multiple flat projections for cross-manifold clustering," *IEEE Transactions on Cybernetics*, vol. 52, no. 8, pp. 7704–7718, 2021.
- [25] N. G. Trillos, P. He, and C. Li, "Large sample spectral analysis of graph-based multi-manifold clustering," *Journal of Machine Learning Research*, vol. 24, no. 143, pp. 1–71, 2023.
- [26] S. Boral, S. Dhar, and A. Ghosh, "Unsupervised segmentation of non-intersecting manifolds," in *The 12th International Conference on Advances in Information Technology*, 2021, pp. 1–7.
- [27] F. Murtagh and P. Contreras, "Algorithms for hierarchical clustering: an overview," *Wiley Interdisciplinary Reviews: Data Mining and Knowledge Discovery*, vol. 2, no. 1, pp. 86–97, 2012.
- [28] F. Camastra and A. Staiano, "Intrinsic dimension estimation: Advances and open problems," *Information Sciences*, vol. 328, pp. 26–41, 2016. [Online]. Available: <https://www.sciencedirect.com/science/article/pii/S0020025515006179>
- [29] D. Haynes, S. Corns, and G. K. Venayagamoorthy, "An exponential moving average algorithm," in *2012 IEEE Congress on Evolutionary Computation*. IEEE, 2012, pp. 1–8.
- [30] K. Nakai, "Ecoli," UCI Machine Learning Repository, 1996, DOI: <https://doi.org/10.24432/C5388M>.
- [31] S. Aeberhard and M. Forina, "Wine," UCI Machine Learning Repository, 1991, DOI: <https://doi.org/10.24432/C5PC7J>.
- [32] M. Bohanec, "Car Evaluation," UCI Machine Learning Repository, 1997, DOI: <https://doi.org/10.24432/C5JP48>.
- [33] "Echocardiogram," UCI Machine Learning Repository, 1989, DOI: <https://doi.org/10.24432/C5QW24>.
- [34] V. Sigillito, S. Wing, L. Hutton, and K. Baker, "Ionosphere," UCI Machine Learning Repository, 1989, DOI: <https://doi.org/10.24432/C5W01B>.
- [35] "Hepatitis," UCI Machine Learning Repository, 1988, DOI: <https://doi.org/10.24432/C5Q59J>.
- [36] R. Forsyth, "Zoo," UCI Machine Learning Repository, 1990, DOI: <https://doi.org/10.24432/C5R59V>.
- [37] M. Charytanowicz, J. Niewczas, P. Kulczycki, P. Kowalski, and S. Łukasik, "Seeds," UCI Machine Learning Repository, 2012, <https://doi.org/10.24432/C5H30K>.
- [38] R. Quinlan, "Statlog (Australian Credit Approval)," UCI Machine Learning Repository, DOI: <https://doi.org/10.24432/C59012>.
- [39] R. A. Fisher, "Iris," UCI Machine Learning Repository, 1988, DOI: <https://doi.org/10.24432/C56C76>.
- [40] D. Slate, "Letter Recognition," UCI Machine Learning Repository, 1991, DOI: <https://doi.org/10.24432/C5ZP40>.
- [41] N. S. Chauhan, "DNA Sequence Dataset," accessed: 2024-09-30.
- [42] R. Cole and M. Fanty, "ISOLET," UCI Machine Learning Repository, 1994, DOI: <https://doi.org/10.24432/C51G69>.
- [43] "Swarm Behaviour," UCI Machine Learning Repository, 2020, DOI: <https://doi.org/10.24432/C5N02J>.
- [44] J. M. Santos and M. Embrechts, "On the use of the adjusted rand index as a metric for evaluating supervised classification," in *International conference on artificial neural networks*. Springer, 2009, pp. 175–184.
- [45] R. Koopman and S. Wang, "Mutual information based labelling and comparing clusters," *Scientometrics*, vol. 111, no. 2, pp. 1157–1167, 2017.
- [46] M. R. Sheldon, M. J. Fillyaw, and W. D. Thompson, "The use and interpretation of the friedman test in the analysis of ordinal-scale data in repeated measures designs," *Physiotherapy Research International*, vol. 1, no. 4, pp. 221–228, 1996.
- [47] R. F. Woolson, "Wilcoxon signed-rank test," *Wiley encyclopedia of clinical trials*, pp. 1–3, 2007.



Subhadip Boral received the M. Sc. in Computer Science degree from West Bengal State University in 2016. He is presently working as a Research Fellow at the Technology Innovation Hub at Indian Statistical Institute. His current research interests include Unsupervised Learning, Dimensionality Reduction, Streaming Data Analysis, and Anomaly Detection.



Rikathi Pal completed her B.Tech in Information Technology from the University of Calcutta, Kolkata. She is currently a Pre-doctoral Research Fellow at the Indian Institute of Science (IISc), Bangalore. Her research focuses on image segmentation and the theoretical understanding of neural network training processes through topological data analysis (TDA).



Ashish Ghosh is a Senior Professor at the Indian Statistical Institute. He has published more than 270 research papers in international journals and conferences, and acting as the Principal Investigator of several funded projects. His current research interests include Machine and Deep Learning, Data Science, Image/Video Analysis, and Computational Intelligence.